Desalination and Water Treatment
www.deswater.com
doi: 10.5004/dwt.2021.27900

244 (2021) 279–290
December

Methyl orange dye removal from wastewater by novel developed chitosan Schiff bases

S. Aboulhadeed[a], H.M. Ahmed[a], R.E. Khalifa[a], A.M. Omer[a], T.M. Tamer[a], A. Abdelkhalek[b], M.S. Mohy-Eldin[a,*]

[a]*Polymer Materials Research Department, Advanced Technologies and New Materials Research Institute, City of Scientific Research and Technological Applications (SRTA-City), New Borg El-Arab City, P.O. Box: 21934, Alexandria, Egypt, Tel. +2034593414; emails: mmohyeldin@srtacity.sci.eg (M.S. Mohy-Eldin), s.a.aboulhadeed@gmail.com (S. Aboulhadeed), malak.scientist@gmail.com (H.M. Ahmed), randaghonim@gmail.com (R.E. Khalifa), amomar@srtacity.sci.eg (A.M. Omer), tmahmoud@srtacity.sci.eg (T.M. Tamer)*
[b]*Plant Protection and Biomolecular Diagnosis Department, ALCRI, City of Scientific Research and Technological Applications (SRTA-City), New Borg El-Arab City, P.O. Box: 21934, Alexandria, Egypt, email: aabdelkhalek@srtacity.sci.eg*

Received 28 May 2021; Accepted 7 October 2021

ABSTRACT

The impact of synthetic dyes from wastewaters decreases using various methods developed to remove these dyes via a clean and safe process. The current work aimed to modify the chitosan structure as a linear cationic polymer to improve its behaviour via preparing two different crosslinked chitosan Schiff bases hydrogels using a glutaraldehyde crosslinker. The chitosan was coupled with succinimide (Ch/Su) and 1-methyl-2-pyrrolidinone (Ch/Mp). The Schiff bases hydrogels properties such as water uptakes and ion exchange capacity were examined. Fourier transform infrared spectroscopy (FT-IR), scanning electron microscopy (SEM), and thermal analysis (DSC and TGA) were used to investigate the change in their properties. The adsorption of methyl orange (MO) dye from aqueous solutions by the prepared crosslinked chitosan Schiff bases (Ch/Su) and (Ch/Mp) was carried in dynamic batch mode compared to crosslinked chitosan native (Ch). The effect of contact time, initial dye concentration, temperature, system pH, agitation rate, dye concentration, and adsorbent dosage on the MO adsorption was investigated. A rapid MO adsorption process for chitosan derivatives was observed, and the equilibrium reached after only 40 min while the chitosan adsorbent reached equilibrium after 120 min. Typical steady high MO adsorption (%), around 90%, was observed at a wide pH range of the chitosan Schiff bases adsorbents; from 4.0 to 8.0 of Ch/Su and from 4.0 to 9.0 of Ch/Mp adsorbents. The maximum adsorption capacity for the chitosan, Ch/Su and Ch/Mp, at 20ppm MO, was found 8.867, 10.0, and 7.2 mg/g, respectively. Furthermore, statistical analyses of the impact of the adsorption conditions on the MO dye removal (%) were performed.

Keywords: Chitosan; Schiff base; Hydrogel; Anionic dye; Methyl Orange.

1. Introduction

The accelerated growth of world populations raises the need for regenerative water resources. The progress for many industries, especially the textile ones, depends mainly on consuming large amounts of water and coloured wastewater resulted at the end, which proposed the reuse of wastewater as a logical solution to respond to the continuous water demands. The resulted wastewater from textile industries mainly has low transparency and is coloured

* Corresponding author.

caused by very few amounts of dyes [1,2]. It is estimated that 10–15% of the dye is lost in the effluent during the dyeing process [3–5]. The anionic dyes contribute to the dying processes due to their ability to dye many materials [6–8]. Depending on the materials dying capability, from 10 to 50% of the anionic dyes are released in the wastewaters during the dyeing process [9]. The weak biodegradability of most of the dyes, including the anionic ones, comes mainly from their aromatic moieties and results in an induced serious hazard to aquatic living organisms [10,11]. Selection of the suitable dyes removal technique from a wide range of removal techniques, many factors have to be considered such as the dye environmental impact and hazardous, cost of removal, and the annual released amount. Adsorption shows many advantages nominate it in many cases as one of the best choices [12,13]. Chitosan, among other biosorbents, was investigated as an adsorbent for transition metal ions, organic species as well as coloured material studies [14–19]. They have different functional groups like amino (NH_2) and hydroxyl (OH) groups along their backbone induced simple chemical transformation and modifications [20–23]. Among these modifications, Schiff bases obtained by reaction of free amino groups of chitosan with active carbonyl compounds such as aldehyde or ketone are considered the most accessible transformation [24,25]. The obtained (–RC=N–) groups of these Schiff bases offer several potential analytical and environmental applications by enhancing the adsorption/complexation properties [26,27]. Eco-friendly chitosan Schiff base hydrogel derivatives were synthesized in this research via coupling with succinimide (Ch/Su) and 1-methyl-2-pyrrolidinone (Ch/Mp). The hydrogels' structure was examined and characterized by infrared spectroscopy (FTIR), scanning electron microscopy (SEM), thermal gravimetric analysis (TGA), and differential scanning calorimetry (DSC). The methyl orange, which was tested, differently protonates based on the pH medium, which changed its behaviour and made it challenging to remove effluent. The MO removal by the developed chitosan Schiff bases hydrogels compared to native chitosan was studied via a batch adsorption system under different operational conditions. Furthermore, statistical analyses of the impact of the adsorption conditions on the MO dye removal (%) were performed.

2. Materials and methods

2.1. Materials

Chitosan (molecular weight: 100,000–300,000) was obtained from ACROS Organics™ (USA). Acetic acid (99.8%), hydrochloric acid (37%); pK_a of methyl orange is 3.47 in water at 25°C, succinimide and 1-Methyl-2-pyrrolidinone were all purchased from Sigma-Aldrich (Germany). Sulfuric acid 98 %, sodium hydroxide, and phenolphthalein were purchased from El-Nasr Pharmaceutical Co for Chemicals (Egypt).

2.2. Methods

2.2.1. Preparation of N-functionalized chitosan schiff base

N-functionalized chitosan Schiff bases were performed based on the method in the literature [28]. In detail, (1 g) of the chitosan was dissolved in 50 mL acetic acid solution (2%) at ambient temperature overnight. First, filtration of chitosan solution was carried out using cheesecloth to remove undissolved chitosan. Then a 10 mL of absolute ethanol was added carefully to the chitosan solution, with continuous stirring to have a homogenous solution. Next, 31 mM of succinimide or 1-Methyl-2-pyrrolidinone previously dissolved in 10 mL ethanol was added to the above solution. After that, the temperature was rose to 70°C; the reaction mixture was left to react under continuous stirring for 6 h. Then 5 mL of 10% glutaraldehyde was added to the solution with continuous stirring at 70°C for an additional 1 h. The obtained hydrogels were then cut into small pieces and washed several times with ethanol to remove any un-reacted succinimide or 1-methyl-2-pyrrolidinone, then collected by filtration and finally dried at 60°C under vacuum drying pressure of 65 mbar. The dried hydrogel was grinding well, and particles size between 125–250 μm was collected using gradual mechanical sieving. Two different hydrogels were prepared using succinimide or 1-methyl-2-pyrrolidinone coded as (Ch/Su) and (Ch/Mp). Both Schiff bases were characterized and evaluated comparing to chitosan hydrogel (Ch). The unmodified chitosan hydrogel was prepared under the same conditions without the addition of the aldehyde. The dried chitosan and chitosan Schiff base (Cs/MeB) hydrogels were grinding well, and particles size between 125–250 μm was collected using gradual mechanical sieving for further use in the MO adsorption process.

2.2.2. Swelling experiments

The swelling behaviour of the prepared hydrogel was investigated using distilled water. Accurately weighed amounts of hydrogels were immersed in water and allowed to swell for 24 h at 37°C. The swollen hydrogel was then separated, and the moisture adhered to the surface of hydrogel was removed by blotting them gently in between two filter papers, immediately followed by weighing. The swelling degree of samples was determined according to the following formula [29]:

$$\text{Swelling degree}\,(\%) = \left[\frac{(M_t - M_0)}{M_0}\right] \times 100 \quad (1)$$

where M_t is the weight of the swollen hydrogel and M_0 is the initial dry weight.

2.2.3. Ion exchange capacity of the hydrogel

A known weight of chitosan or Schiff base hydrogels were added to the known volume of 0.1 M H_2SO_4 solution, and the mixture was kept under shaking for three h. Then, the mixture was filtered, and an aliquot was titrated against a standard sodium hydroxide solution. Similarly, control titration without the addition of chitosan was also run. From the difference in the volume of NaOH required for neutralization, the ionic capacity of chitosan samples was calculated using the following equation:

$$\text{Ion exchange capacity(meq/g)} = \frac{(V_2 - V_1)\,A}{W} \quad (2)$$

where V_2 and V_1 are the volumes of NaOH required for complete neutralization of H_2SO_4 in the absence and presence of chitosan membrane, respectively, A is the normality of NaOH and W is the weight of sample taken for analysis [30].

2.2.4. Infrared spectrophotometric

To confirm modification and prove the hydrogel structure, Translucent KBr-discs were prepared by grinding the dried sample materials together with infrared grade KBr and then pressing. FT-IR spectra in the transmittance mode were recorded using FT-IR spectrometer (Shimadzu FTIR-8400 S, Japan), connected to a PC, and analysis the data by IR Solution software, Version 1.21. The FTIR spectrums were obtained by recording 64 scans between 4,000–400 cm^{-1} with a resolution of 2 cm^{-1}.

2.2.5. Thermal gravimetric analysis (TGA)

Analysis by TGA of samples was carried out using a thermogravimetric analyzer (Shimadzu TGA-50, Japan) under Nitrogen to evidence changes in structure due to the modification. Samples were first measured their weight loss starting from room temperature to 600°C at a heating rate of 10°C/min.

2.2.6. Differential scanning calorimeter (DSC)

Differential scanning calorimetric analysis of gelatin and gelatin schiff base samples (~5 mg in sealed Al-pan) was carried out using Differential Scanning Calorimeter device (Shimadzu DSC-60A, Japan) in the temperature range of ambient –500°C at a heating rate of 10°C/min under nitrogen flow (30 mL/min).

2.2.7. Scanning electron microscopic analysis (SEM)

Samples were coated under a vacuum with a thin layer of gold before being examined by scanning electron microscopy. Morphological changes of the sample's surface were followed using a secondary electron detector of SEM under 10 kV and x5000 magnification (Joel JSM 6360LA), Japan.

2.2.8. Batch equilibrium studies

The stock solution of 1 g/L of methyl orange (MO) dye (1,000 ppm) was prepared by dissolving the appropriate amount of dye in distilled water then the used concentrations were obtained by dilution. All the adsorption experiments were conducted in 100 mL flasks by adding a given amount of adsorbent to 25 mL dye solution of different dye concentrations with different pH values and shaking in an orbital shaker for a given time. The adsorbate concentrations in the initial and final aqueous solutions were measured by using UV-Vis spectrophotometer at 465 nm. The amount of dye adsorbed was calculated from the difference between the initial concentration and the equilibrium one. The values of percentage removal and the amount of dye adsorbed were calculated using the following relationships:

$$\text{Dye removal}\left(\%\right)=\frac{\left(C_0-C_e\right)}{C_0}\times 100 \tag{3}$$

where C_0 is the initial dye concentration and C_e is the final dye concentration in supernatant.

2.3. Statistical analyses

Statistical analyses of the impact of the adsorption conditions on the MO dye removal (%) were performed. The analyses were done by one-way analysis of variance (ANOVA) using the CoStat software, and the significant differences were determined according to the least significant difference (LSD). $p \le 0.05$ level of probability. The black color letters indicated the significant differentiation between the individual values of the same treatment (Ch or Ch/Su or Ch/Mp) while, the red color letters indicated the significant differentiation among the three treatments.

3. Results and discussions

In the current research, a new chitosan Schiff base hydrogel was prepared via coupling chitosan amine groups with Succinimide or 1-Methyl-2-pyrrolidinone followed by cross-linking with glutaraldehyde (Fig. 1). The prepared hydrogel was characterized using different characterization tools. The obtained hydrogel was evaluated as a dye removal material using methyl orange as a model for anionic dye.

3.1. Physicochemical characterization

Adsorbent surface charges play an essential role in the formulation of the surface-active site for the adsorption of charged dye. Chitosan function groups such as amine groups originated their cationic nature and its positive charges. Fig. 2 displays the ion exchange capacity of chitosan and its derivatives hydrogels. Decreasing ion exchange capacity from 4.63 of chitosan to 2.74 and 3.58 for (Ch/Su) and (Ch/Mp) respectively confirm consuming chitosan amine groups via coupling with Succinimide and 1 methyl-2 pyrrolidinone. Fig. 2 also shows the decrement of water uptake (%) of the modified chitosan hydrogel than chitosan itself due to the elimination of free amine groups via reaction with carbonyl groups of the succinimide and 1 methyl-2 pyrrolidinone.

3.2. Infrared spectrophotometric (FT-IR)

The FTIR spectra of the chitosan hydrogels are presented in Fig. 3. In the spectrum of chitosan, the broadband at 3,435 cm^{-1} is due to –OH and –NH stretching vibration. 1,627 and 1,587 cm^{-1} bands belong to $-NH_2$ bending. The bands at around 1,635 cm^{-1} represented C=N of glutaraldehyde. The shift of this band and the presence of multi-bands in (Ch/Su) and (Ch/Mp) refer to C=N with succinimide or 1-methyl-2-pyrrolidinone, respectively. The bands occurring at 1,369 cm^{-1} are referred to the C–OH vibration of the primary alcohol groups in the chitosan, and the band around 2,861 cm^{-1} is assigned to the C–H stretching motion in chitosan [31]. The absorption bands at 1,141 cm^{-1} attributed to the skeletal anti-symmetric stretching vibration of C–O–C Bridge and the 1,014 cm^{-1} skeletal vibrations including the C–O stretching are characteristics of its Saccharide structure [32]. In the

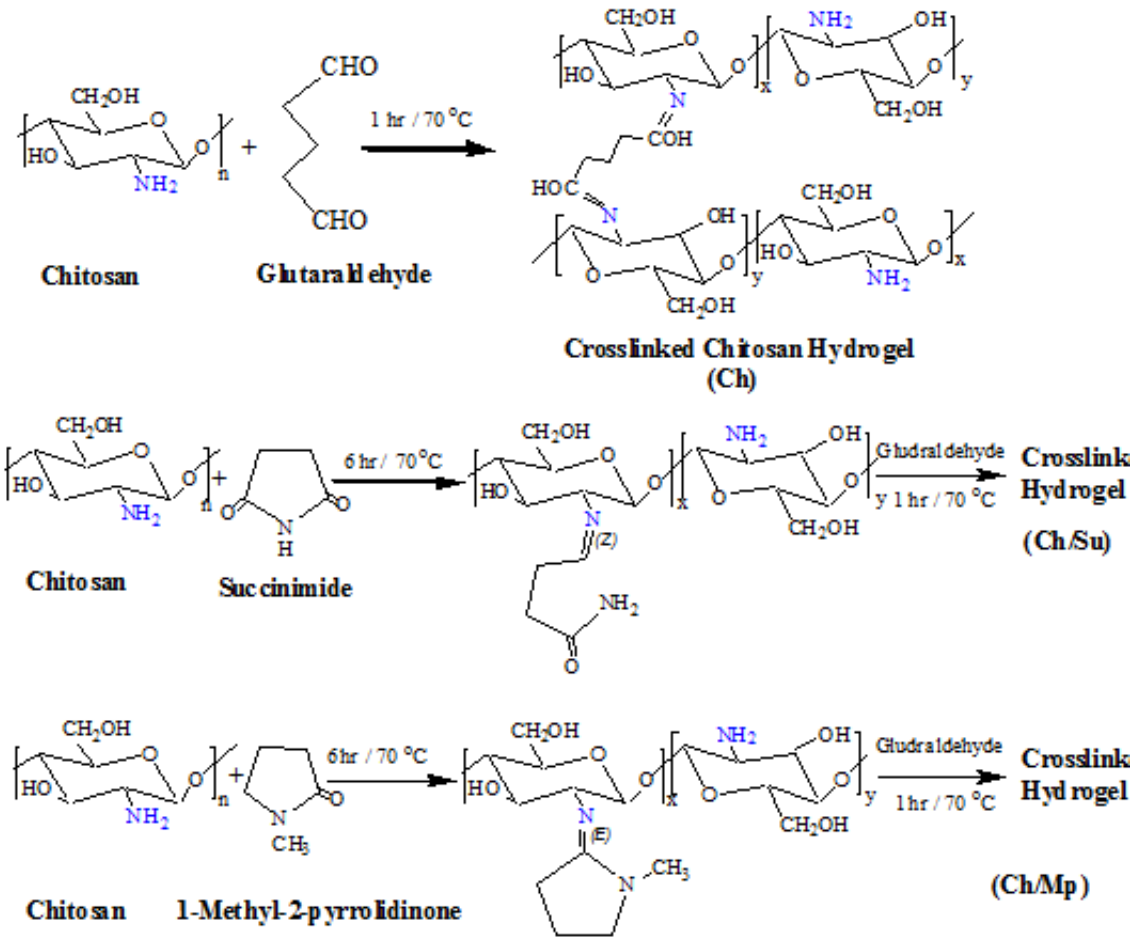

Fig. 1. Schematic preparation of Chitosan, Ch/Su and Ch/Mp Schiff bases hydrogels.

Ch/Su Schiff base, overlapping the characteristic succinimide band at 1,001 cm^{-1} [33] with the 1,014 cm^{-1} skeletal vibrations, including the C–O stretching characteristics of Saccharide structure [32], leads to the appearance of the shifted band at 1,020 cm^{-1}. The more intense band at 1,370 cm^{-1} resulted from the overlapping of the characteristic succinimide band at 1,370 cm^{-1} [33], with the bands occurring at 1,369 cm^{-1} referred to the C–OH vibration of the primary alcohol groups in the Chitosan [28]. The overlapping of the chitosan band around 2,861 cm^{-1} assigned to the C–H stretching motion with the characteristic succinimide band at 2,802 cm^{-1} [33] leads to sharpening of the band. The Ch/Mp Schiff base spectrum [34] shows two characteristics bands of the immobilized 1-methyl-2-pyrrolidinone molecules at 1,300 and 1,700 cm^{-1}. Moreover, the overlapping of the band around 2,861 cm^{-1} is assigned to the C-H stretching motion in chitosan [31] with multiple characteristic bands of the immobilized 1-methyl-2-pyrrolidinone molecules at 2,850–2,980 cm^{-1}, leads to the appearance of a new band at 3,200 cm^{-1}.

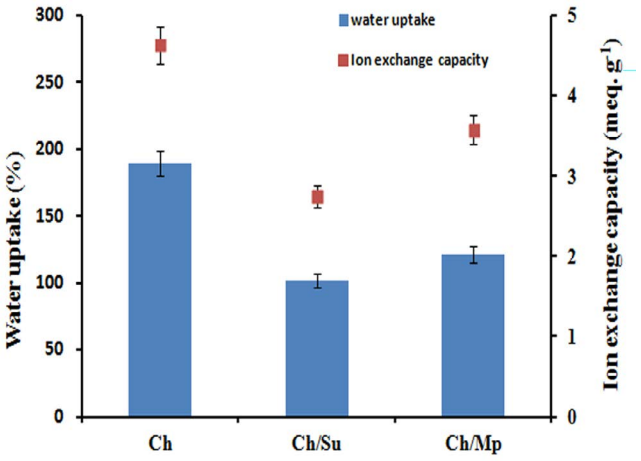

Fig. 2. Water uptake (%) and ion exchange capacity of Chitosan, Ch/Su and Ch/Mp Schiff bases hydrogels.

3.3. Thermal gravimetric analysis (TGA)

The thermal stabilities of the crosslinked chitosan and its Schiff bases derivatives were tested using thermal gravimetric analysis. Chitosan hydrogels exhibited three degradation behaviours in Fig. 4. The 1st weight loss around 100°C that attributed to the elevation of piping water content trapped using hydrophilic groups along the polymer

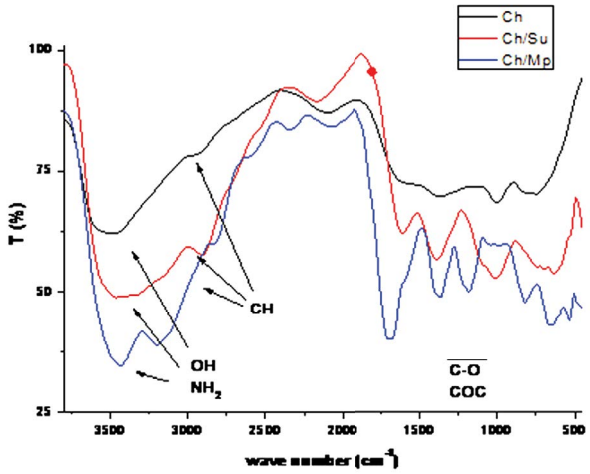

Fig. 3. FT-IR of Chitosan, Ch/Su and Ch/Mp Schiff bases hydrogels.

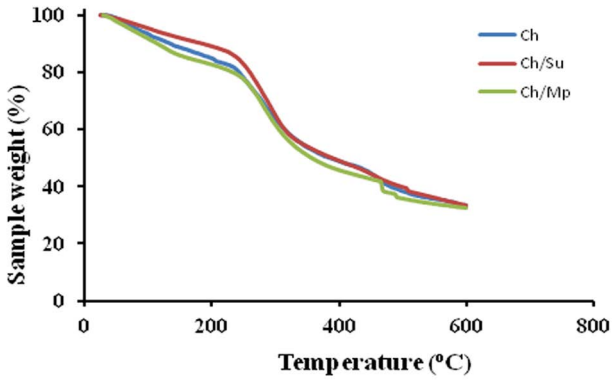

Fig. 4. TGA of Chitosan, Ch/Su and Ch/Mp Schiff bases hydrogels.

backbone (i.e., –OH and –NH_2). Chitosan and its Schiff bases derivatives demonstrate lower water content than its Schiff base hydrogels with 11.41%, 7.8% and 14.1% for CH, Ch/Su and Ch/Mp Schiff bases, respectively at 150°C. That can be explained by the higher possibility of the Ch/Su Schiff base crosslinking and the pseudo hydrophilic nature of the Ch/Mp Schiff base [35]. The 2nd weight depression was recognized at 220°C–320°C. That refers to distractive degradation of the chitosan glucose ring [36]. Finally, the loss of 50% of tested samples at 385.88°C, 388.5°C and 356°C for CH, Ch/Su and Ch/Mp Schiff bases, respectively, indicate the non-significant effect of Ch/Su Schiff base formation on the thermal stability of the hydrogel. That observation could be attributed to keeping the formed Ch/Su Schiff base with the same number of amine groups as native chitosan (Fig. 1), which is mainly responsible for the thermal stability of chitosan and the formed Ch/Su Schiff base, keeping in mind the dependence of the glutaraldehyde crosslinking step on the number of the amine groups.

On the other hand, the Ch/Mp Schiff bases show less thermal stability with lower 30°C than chitosan and Ch/Su Schiff base to lose 50% of their weight. The consumption of the amine groups during the Ch/Mp Schiff base formation consequently reduced the crosslinking degree with glutaraldehyde and, accordingly, the thermal stability. The 3rd degradation stage at a higher temperature has resulted from the degradation of the formed residue in the previous step [36].

3.4. Differential scanning calorimetry (DSC)

Fig. 5 depicts the DSC curves for Chitosan, Ch/Su, and Ch/Mp hydrogel. In all these curves, an endothermic peak around 75°C can be described by the illumination of moisture associated with the hydrophilic groups of the hydrogels [37,38]. The second thermal shift may be associated with the destruction of amine in glucosamine units with correspondent exothermic from 220°C–320°C [39].

3.5. Scanning electron microscope (SEM)

The morphological structure of chitosan, (Ch/Su) and (Ch/Mp) hydrogels were investigated using a scanning electron microscope and presented in Fig. 6. Relative to the chitosan surface morphology, the Ch/Su surface shows a porous surface structure, while new fibres structures have more noticeable Ch/Mp surface morphology changes. That can be illustrated by the appearance of the incompatible side chain. These chains increase the spacing between polymer chains. In addition, replacing hydrophilic amine groups with hydrophobic aromatic groups can distort the crystal structure of polymer [40].

3.6. Adsorption process

In this work, we investigated the sorption behaviour of chitosan and its Schiff base hydrogels which give the maximum removal per cent and its applicability to artificially contaminated water with methyl orange (MO) solution. A batch experiment will be performed in which aqueous solutions of the MO were prepared. The adsorption behaviours of the hydrogels towards the MO were optimized under different adsorption conditions of time, temperature, dye pH, agitation rate and, adsorbent dosage.

3.7. Effect of time

Fig. 7 displays the effect of variation of adsorption time of the adsorption process of MO on chitosan and its derivatives. Increased contact time demonstrates a rapid increase in the adsorption process until 40 min and then going to the equilibrium phase for chitosan derivatives while chitosan slowly reaches equilibrium phase after 120 min. This phenomenon can be referred to as an increase in the adsorption capacity of chitosan by Schiff base formation. Although the cationic charge of chitosan was partially consumed due to Schiff bases formation, it is expected to have lower adsorption capacity. The click grafting of 1 methyl-2 pyrrolidinone with hydrophobic methyl groups onto the chitosan backbone increases the surface roughness. It offers a higher surface area for the hydrophobic-hydrophobic interaction, which added physical adsorption to the chemical one and having a positive synergetic impact on the adsorption rate at the early adsorption stage.

On the other hand, the click grafting of succinimide does not reduce the number of the free amine groups which replaced the original C2 amine groups with remote ones which are more accessible to the MO dye molecules in the solution and accordingly have the highest adsorption rate in the early adsorption process stage where 97% of MO dye removed after only 40 min. Despite the chitosan Schiff bases adsorbents formed via converting their primary amino groups to tertiary ones, the Schiff base nitrogen in the created structures is still capable of protonation. However, protonated Schiff bases were compromised by the grafted hydrophobic groups' effect in the chitosan-1-methyl-2 pyrrolidinone Schiff base and the steric hindrance in the case of chitosan-succinimide Schiff base.

3.8. Effect of temperature

The effect of environmental temperature on the adsorption process of MO on tested hydrogels was measured from 25 to 80°C and presented in Fig. 8. There is a significant increase of dye adsorption on chitosan hydrogel by increased temperature, where it was slightly influenced in Schiff base derivatives that can be explained by the presence of highly active adsorption sites compared to dye molecules in the tested solution [41,42].

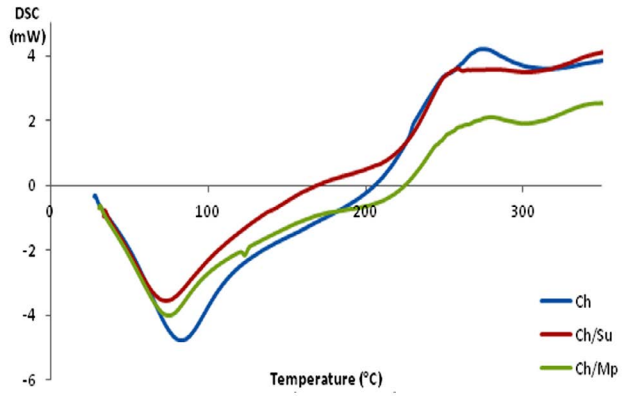

Fig. 5. DSC of Chitosan, Ch/Su and Ch/Mp Schiff bases hydrogels.

3.9. Effect of agitation

The effect of the agitation rate on the adsorption process was investigated at various agitation rates (50–250 rpm). Fig. 9 shows an increase in adsorption capacity of chitosan and its hydrogel derivatives by increase agitation rate until 150 rpm. Further increase in agitation shows a slight improvement of MO adsorption. Increase the agitation rate simplified diffusion of MO molecules to the adsorbent surface. Thus increasing the stir rate will eliminate the thickness of the liquid layer and the mass-transfer resistance for the adsorbent samples. Therefore, these also mean that 150 rpm is sufficient to ensure that all the surface binding sites are readily available for methyl orange uptake [43,44].

3.10. Effect of pH

The pH is estimated as a critical parameter in adsorption investigations as it controls the adsorption process at the adsorbent solution interface. It influences both the active adsorbent sites and the dye molecules charges. Experiments

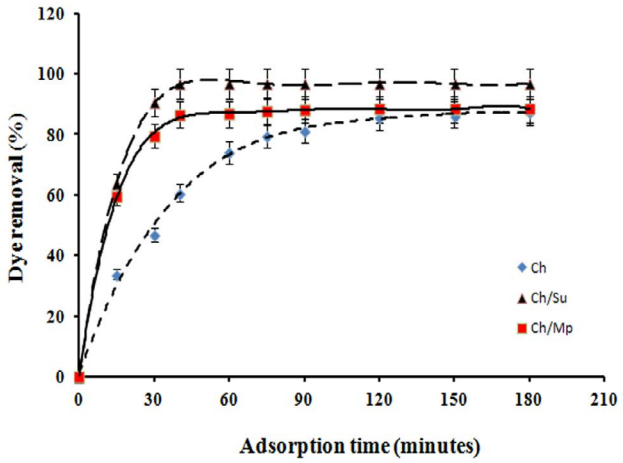

Fig. 7. Effect of the adsorption' time on the removing percent (%) of MO using Chitosan, Ch/Su and Ch/Mp Schiff bases hydrogels; [25 mL of 10 ppm MO, pH 4.0, 0.2 g adsorbent, temperature 60°C, 250 rpm].

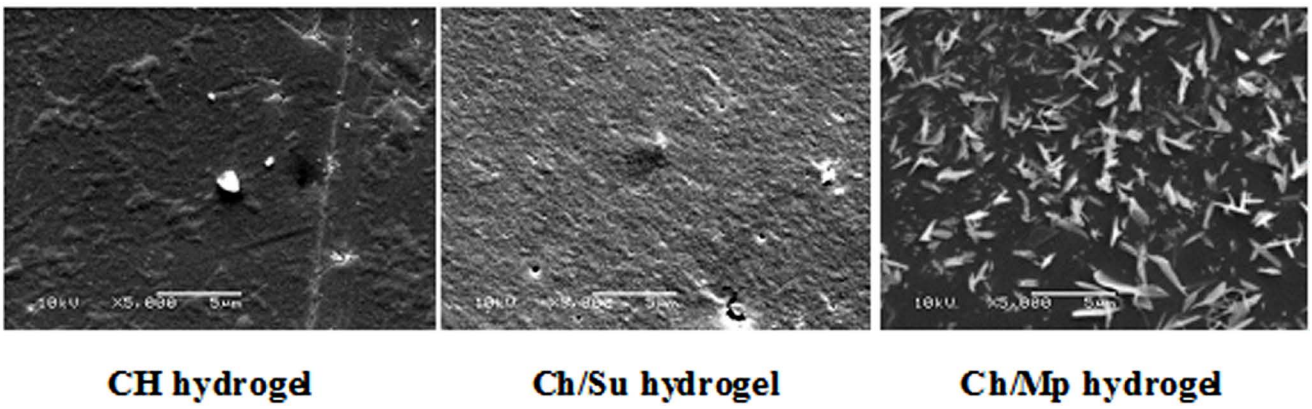

Fig. 6. SEM pictures of Chitosan, Ch/Su and Ch/Mp Schiff bases hydrogels.

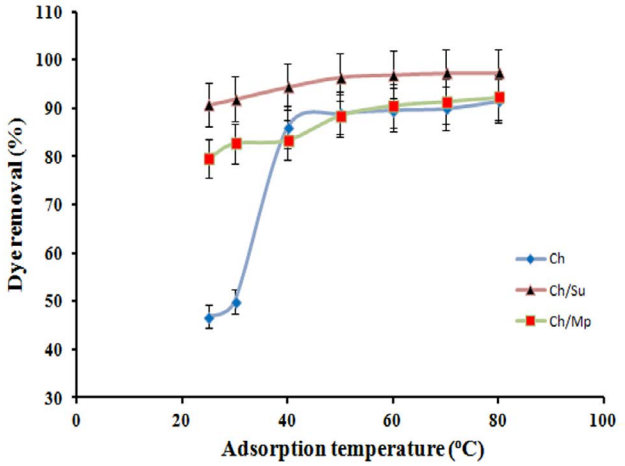

Fig. 8. Effect of the adsorption' temperature on the removing percent (%) of MO using Chitosan, Ch/Su and Ch/Mp Schiff bases hydrogels; [25 mL of 10 ppm MO, pH 4.0, 0.2 g adsorbent, time 120 min, 250 rpm].

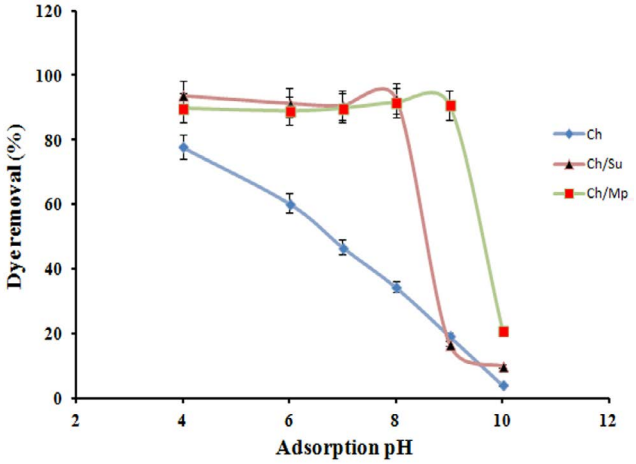

Fig. 10. Effect of the solution pH on the removing percent (%) of MO using Chitosan, Ch/Su and Ch/Mp Schiff bases hydrogels; [25 mL of 10 ppm MO, 250 rpm, 0.2 g adsorbent, time 120 min, temperature 60°C].

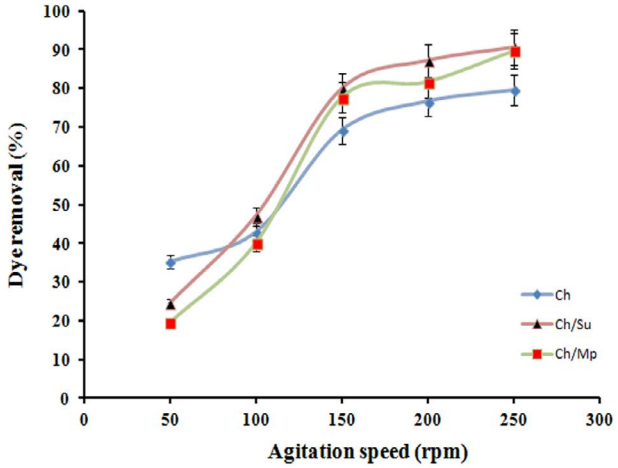

Fig. 9. Effect of agitation rate on the removing percent (%) of MO using Chitosan, Ch/Su and Ch/Mp Schiff bases hydrogels; [25 mL of 10 ppm MO, pH 4.0, 0.2 g adsorbent, time 120 min, temperature 60°C].

were carried out at varying the solution pH from 4 to 10 while the rest were kept constant. The maximum removal of MO dye on chitosan hydrogels was observed at pH 4.0, as illustrated in Fig. 10. That can explain by the cationic nature of chitosan at acidic pH. That generates a favourite positive active side for anionic dye (i.e., MO). With further increase of the medium pH beyond pH 4.0, different behaviours' observed for the chitosan and chitosan Schiff base adsorbents. For chitosan adsorbent, a linear decrement of the MO dye removal percentage was observed due to the continuous deprotonation of the amine groups and consequently the water content and the available number of positive adsorption sites.

On the other hand, chitosan Schiff base derivatives demonstrate different behaviours, showing steady MO dye removal (%) in the neutral and slightly alkaline environment to pH 8.0 of Ch/Su and pH 9.0 of Ch/Mp Schiff bases hydrogels. A sharp decline of the MO removal (%) of Ch/Su Schiff bases hydrogel was observed from 92.7% at pH 8.0 to 17% and 10% at pH 9.0 and pH 10.0, respectively. While a sharp decline of the MO removal (%) Ch/Mp Schiff bases hydrogel was observed from 90.84% at typical to 21% at pH 10.0. The joint steady adsorption pH range from 6.0 to 8.0 of the Chitosan Schiff bases adsorbents can be explained by two reasons. The first is the reduced number of the free amine groups' numbers affected by the deprotonation. The second is to increase the physical adsorption role of the chitosan Schiff bases adsorbents via hydrophobic-hydrophobic interaction, which is expected to be higher in the Ch/Mp Schiff base hydrogel containing heterocyclic ring with an attached methyl group.

3.11. Effect of absorbent dose

The influence of adsorbent dose on MO removal was studied by changing the adsorbent amount from 0.025 to 0.2 g. The observed trend due to variation in chitosan and its Schiff base derivatives hydrogels dose is represented in Fig. 11. The adsorption rate increased with the rise in adsorbent dose due to additional active sites being available for dye adsorption [45,46]. However, it was also observed that after particular addition of dose, the adsorption of the dye remains constant with a further addition in adsorbent dose, which implied that the MO concentration gradient between the liquid phase (MO solution) and the solid phase (adsorbent) almost disappeared and consequently the driving force to move the MO molecules towards the adsorbent surface lost.

3.12. Effect of MO concentration

Fig. 12 shows the effect of initial MO concentration on the removing per cent (%). Three general observations have

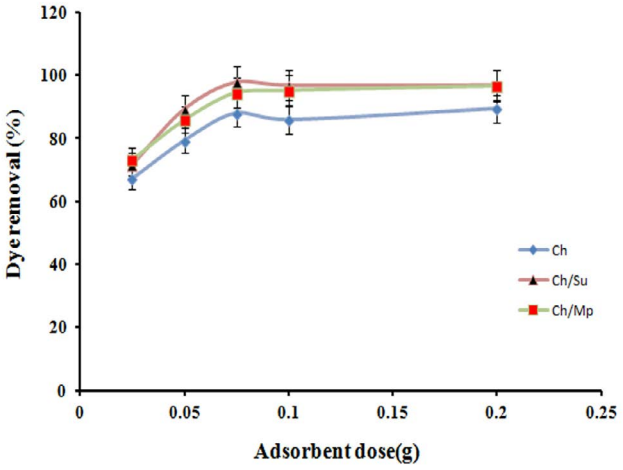

Fig. 11. Effect of adsorbent dose on the removing percent (%) of MO using Chitosan, Ch/Su and Ch/Mp Schiff bases hydrogels; [25 mL of 10 ppm MO, pH 4.0, time 120 min, temperature 60°C, 250 rpm].

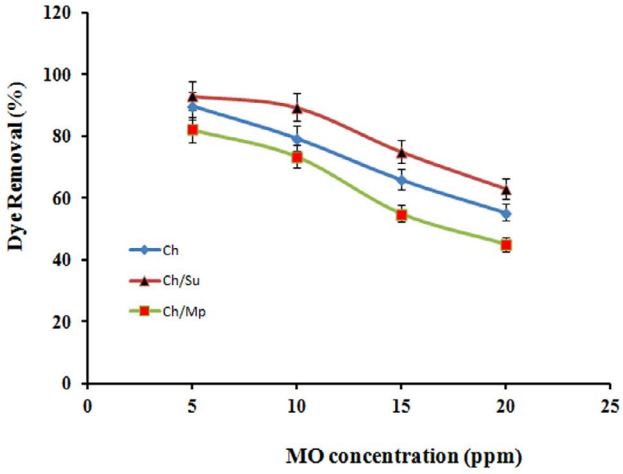

Fig. 12. Effect of the MO concentration on their removing percent (%) using Chitosan and Ch/Su, Ch/Mp Schiff bases hydrogels; [25 mL of MO, pH 4.0, 0.2 g adsorbent, time 120 min, temperature 60°C, 250 rpm].

been recognized. The first observation concerns the close removal percentages of all adsorbents at MO 5ppm. The second observation concerns the decline behaviour of the removal percentage with an increase of the initial MO concentrations. The third observation is the order of the adsorbents based on their removal percentage behaviour as follow; Ch/Su, Ch and Ch/Mp, respectively.

In chitosan adsorbent, the removal percentage linearly reduced at an almost average rate of 11%, from 5 to 20 ppm. This trend is due to the consumption of the limited number of protonated amine groups' active sites in the interaction with the negatively charged MO molecules. With further increase of the MO concentration, an electrostatic repulsion between the adsorbed MO molecules over the chitosan surface and the left ones in the solution phase. A similar effect was observed with the other anionic dyes [6,22,46,47]. Different behaviour of the chitosan derivate Schiff bases was obtained where two MO removal percentage stages have been recognized. In the first stage, from 5ppm to 10 ppm, the Ch/Su and Ch/Mp lost 4% and 8.5% of their removal percentages. From 10 to 15 ppm, the second stage lost 15% and 18% of its adsorption removal percentages. While from 15 to 20 ppm, the Ch/Su and Ch/Mp lost 12% and 10%. In the case of the Ch/Su adsorbent, although the Schiff base formation does not affect the number of the amine groups according to Fig. 1, it has a higher MO removal percentage than chitosan. This behaviour may be referred to as the contribution of the hydrophobic-hydrophobic interaction and more offered pores internal surface area due to the incorporation of the remote amide groups of the formed Schiff base in the cross-linking process glutaraldehyde. On the other hand, the Ch/Mp adsorbent has the lowest adsorption capability, which shows a lower removal percentage than the chitosan adsorbent. The interaction of the MO molecules with the left free amine groups has a prominent contribution role in the removal process. It is worthy of mentioning here that the Ch/Mp adsorbent has an 8.3% Mo removal percentage less relative to the chitosan adsorbent at MO 5ppm. Assuming that the removal mechanism is referred only to the interaction between the protonated amine groups and the MO molecules, the Ch/Mp adsorbent should have a 33.2% MO removal percentage less relative to the chitosan adsorbent at MO 20ppm. The Ch/Mp adsorbent has only18.8% Mo removal percentage less than the chitosan adsorbent at MO 20ppm. This finding implies the additional contribution of hydrophobic-hydrophobic interaction between the methyl and the pyrrolidinone attached groups and the aromatic rings and the methyl groups of the MO molecule.

The obtained results follow the previously published result by the authors using Chitosan derivate Schiff bases obtained from the coupling of chitosan with 1-vinyl 2- pyrrolidone and 4-amino acetanilide [48]. The maximum adsorption capacity for the Chitosan, Ch/Su and Ch/Mp, at 20 ppm MO, were compared with the literature and provided in Table 1 [48–52].

3.13. Statistical analysis

Statistical analyses of the impact of the adsorption conditions on the MO dye removal (%) were performed and the obtained data presented in Table 2. For the adsorption time parameter, it was shown that the adsorption value for Ch treatment increased with time increasing where the highest adsorption value (87.28%) was exhibited at 180 min. On the other hand, the highest adsorption values (96.78% and 88.14%) were observed at 40 and 90 min for Ch/Su and Ch/MP, respectively (Table 2). After these two times, there is no significant changes were reported. Interestingly, at all adsorption times studied, the Ch/Su treatment showed the highest values followed by Ch/MP and Ch/Mp (Table 2).

For the adsorption temperature parameter, the adsorption value of both Ch and Ch/Mp treatments increased with time increasing reaching the highest value of 91.35% and 92.20%, respectively, at 80°C (Table 2). Although the highest adsorption value of Ch/Su treatment (97.29%) was observed

Table 1
Adsorption capacities (AC; mg/g) of MO on different adsorbents

Adsorbent	AC (mg/g)	References
Chitosan Schiff bases (I & II)	1.20 and 10.70	48
Ferric oxide–biochar nano-composites derived from pulp and paper sludge	16.05	49
NiO NP_s	11.21	50
Novel magnetic CNTs/Fe@C	16.53	51
Functionalized-CNTs loaded TiO_2	42.85	52
Chitosan	8.87	This work
Ch/Su Schiff base	10.00	This work
Ch/Mp Schiff base	7.20	This work

at 80°C, there is no significant change was reported at 50°C, 60°C and 70°C ($p \leq 0.05$). Similar to the adsorption time parameter, Ch/Su treatment showed that highest values at all temperatures studied followed by Ch/MP except at 40°C and 50°C (Table 2).

For the adsorption pH parameter, both Ch and Ch/Su treatments exhibited the highest adsorption values (77.80% and 93.73%) at pH 4, respectively, then decreased gradually reaching the lowest values at pH 10 (Table 2). On the other hand, Ch/Mp treatment showed the highest adsorption value (91.53%) at pH 8 with no significant change at pH 9 value (90.85%). At the first four pH degrees (4, 6, 7, and 8) the Ch/Su treatment showed the highest adsorption value followed by Ch/Mp and Ch treatments, while at pH 9 and 10 the Ch/Mp treatment exhibited the highest adsorption values followed by Ch and Ch/Su treatments (Table 2).

For the agitation rpm parameter, it was observed that the rpm increases were associated with significant adsorption value increasing for all treatments. At 50 rpm, the Ch treatment showed the highest adsorption value followed by Ch/Su and Ch/Mp treatments (Table 2). After that, the Ch/Su treatment exhibited the highest adsorption value followed by Ch/Mp and Ch at all studied rpm except at 100 rpm that showed a higher Ch adsorption value (Table 2).

For the adsorption dose parameter, it was showed that there is no significant change in adsorption values between 0.075 and 0.2 g for Ch treatment, and between 0.1 and 0.2 g for both Ch/Su and Ch/Mp treatments. Both 0.075 and 0.2 g exhibited the highest adsorption value for Ch treatment. For Ch/Su treatment 0.075 showed the highest adsorption value while 0.2 g exhibited the highest adsorption value for Ch/Mp treatment (Table 2). At two adsorption doses (0.025 and 0.05 g) the Ch/Mp treatment showed significant adsorption values followed by Ch/Su and Ch treatments. By increasing adsorption dose, Ch/Su exhibited the greatest adsorption values at 0.075, 0.1 and 0.2 g compared to the other two treatments at $p \leq 0.05$ (Table 2).

For Mo concentration parameter, it was observed that the increasing Mo conc. Were associated with decreasing adsorption value for all treatments (Table 2). All individual values showed significant differences at all Mo concentrations. Among three treatments, the Ch/Su treatment exhibited a significant adsorption value followed by Ch/Mp and Ch treatments at all concentrations.

4. Conclusion

Novel crosslinked chitosan Schiff base derivates were developed by coupling chitosan with succinimide and 1-methyl-2-pyrrolidinone to have (Ch/Su) and (Ch/Mp) Schiff bases adsorbents for the removal of methyl orange, anionic dye, from aqueous solutions. The developed Ch/Su Schiff base adsorbent bearing terminal primary amine groups instead of the chitosan ones formed the Schiff base and acquired a porous structure. On the other hand, the developed Ch/Mp Schiff base adsorbent bearing terminal methyl-2-pyrrolidinone groups induced extra hydrophobicity. That explains the high-speed adsorption rate of the MO by the chitosan Schiff base derivates where the equilibrium attained after only 40 min compared with 120 min for chitosan. The adsorbents have been ordered based on their removal percentage behaviour: Ch/Su, Ch and Ch/Mp, respectively. In the case of the Ch/Su adsorbent, although the Schiff base formation does not affect the number of the amine groups according to Fig. 1, it has a higher MO removal percentage than chitosan. This behaviour may be referred to as the contribution of the hydrophobic-hydrophobic interaction and more offered pores internal surface area due to the incorporation of the remote amide groups of the formed Schiff base in the crosslinking process glutaraldehyde.

On the other hand, the Ch/Mp adsorbent has the lowest adsorption capability, which shows a lower removal percentage than the chitosan adsorbent. The interaction of the MO molecules with the left free amine groups has a prominent contribution role in the removal process. An additional contribution of hydrophobic-hydrophobic interaction between the methyl and the pyrrolidinone attached groups and the aromatic rings and the methyl groups of the MO molecule have been observed. Within the studied range of MO concentration, the developed chitosan Schiff bases hydrogels show a constant adsorption ability over wide ranges of temperature (40°C–80°C) and pH (4.0–8.0) for the Ch/Su Schiff base and pH (4.0–9.0) for the Ch/Mp Schiff base of the wastewater. The obtained behavior nominates the developed chitosan Schiff bases hydrogels to work under a wide range of operational pH and temperature conditions. Furthermore, statistical analyses of the impact of the adsorption conditions on the MO dye removal (%) were performed.

Table 2
Effect of different adsorption parameters on different treatments

Adsorption time				Adsorption Temp				Adsorption pH			
Time (min)	Ch	Ch/Su	Ch/Mp	Temp. (°C)	Ch	Ch/Su	Ch/Mp	pH	Ch	Ch/Su	Ch/Mp
0	00.00 *i*	00.00 *d*	00.00 *f*	25	46.78 *e* – c	90.68 *d* – *a*	79.49 *e* – *b*	4	77.80 *a* – *c*	93.73 *a* – *a*	89.83 *bc* – *b*
15	33.90 *h* – *c*	63.73 *c* – *a*	59.49 *e* – *b*	30	50.00 *d* – c	91.86 *c* – *a*	82.71 *d* – *b*	6	60.34 *b* – *c*	91.36 *b* – *a*	88.98 *c* – *b*
30	46.78 *g* – *c*	90.68 *b* – *a*	79.49 *d* – *b*	40	86.10 *c* – b	94.41 *b* – *a*	83.39 *d* – *c*	7	46.78 *c* – *c*	90.68 *b* – *a*	89.83 *bc* – *b*
40	60.68 *f* – *c*	96.78 *a* – *a*	86.61 *c* – *b*	50	88.98 *b* – b	96.44 *a* – *a*	88.47 *c* – *c*	8	34.41 *d* – *c*	92.71 *a* – *a*	91.53 *a* – *b*
60	74.07 *e* – *c*	96.78 *a* – *a*	86.78 *bc* – *b*	60	89.66 *b* – c	96.95 *a* – *a*	90.51 *b* – *b*	9	19.32 *e* – *b*	16.95 *c* – *c*	90.85 *ab* – *a*
75	79.66 *d* – *c*	96.78 *a* – *a*	87.63 *ab* – *b*	70	90.00 *ab* – c	97.29 *a* – *a*	91.36 *ab* – *b*	10	04.07 *f* – *b*	10.00 *d* – *c*	21.02 *d* – *a*
90	81.19 *c* – *c*	96.78 *a* – *a*	88.14 *a* – *b*	80	91.53 *a* – c	97.29 *a* – *a*	92.20 *a* – *b*				
120	85.76 *b* – *c*	96.78 *a* – *a*	88.31 *a* – *b*								
150	86.44 *ab* – *c*	96.78 *a* – *a*	88.31 *a* – b								
180	87.29 *a* – *c*	96.78 *a* – *a*	88.31 *a* – b								
Agitation rpm				Adsorption dose				Mo concentration			
rpm	Ch	Ch/Su	Ch/Mp	sample(gm)	Ch	Ch/Su	Ch/Mp	MO	Ch	Ch/Su	Ch/Mp
50	35.25 *e* – *a*	24.41 *e* – *b*	19.49 *e* – *c*	0.025	67.29 *d* – *c*	71.69 *d* – *b*	73.39 *d* – *a*	5	89.66 *a* – *b*	93.00 *a* – *a*	82.2 *a* – *c*
100	42.88 *d* – *b*	46.95 *d* – *a*	40.00 *d* – *c*	0.05	79.32 *c* – *c*	89.32 *c* – *b*	85.93 *c* – *a*	10	79.32 *b* – *b*	89.32 *b* – *a*	73.56 *b* – *c*
150	69.15 *c* – *c*	79.83 *c* – *a*	77.63 *c* – *b*	0.075	87.97 *a* – *c*	97.80 *a* – *a*	94.58 *b* – *b*	15	66.00 *c* – *b*	75.00 *c* – *a*	55.00 *c* – *c*
200	76.61 *b* – *c*	87.12 *b* – *a*	81.69 *b* – *b*	0.1	85.76 *b* – *c*	96.78 *b* – *a*	95.25 *ab* – *b*	20	55.42 *d* – *b*	63.00 *d* – *a*	45.00 *d* – *c*
250	79.49 *a* – *c*	90.51 *a* – *a*	89.66 *a* – *b*	0.2	89.32 *a* – *c*	96.78 *b* – *a*	96.61 *a* – *b*				

The black color letters indicated the significant differentiation between the individual values of the same treatment (Ch or Ch/Su or Ch/Mp) while, the red color letters indicated the significant differentiation among the three treatments. Data with the same letters are not significantly different at $p \leq 0.05$.

References

[1] I.M. Banat, P. Nigam, D. Singh, R. Marchant, Microbial decolourization of textile-dyecontaining effluents: a review, Bioresour. Technol., 58 (1996) 217–227.

[2] T. Robinson, G. McMullan, R. Marchant, P. Nigam, Remediation of dyes in textile effluent: a critical review on current treatment technologies with a proposed alternative, Bioresour. Technol., 77 (2001) 247–255.

[3] V.K. Gupta, B. Gupta, A. Rastogi, S. Agarwal, A. Nayak, Pesticides removal from wastewater by activated carbon prepared from waste rubber tire, Water Res., 45 (2011) 4047–4055.

[4] V.K. Gupta, R. Jain, A. Nayak, S. Agarwal, M. Shrivastava, Removal of the hazardous dye-tartrazine by photodegradation on titanium dioxide surface, Mater. Sci. Eng., C, 31 (2011) 1062–1067.

[5] K. Gupta, R. Jain, T.A. Saleh, A. Nayak, S. Malathi, S. Agarwal, Equilibrium and thermodynamic studies on the removal and recovery of Safranine-T Dye from industrial effluents, Sep. Sci. Technol., 46 (2011) 839–846.

[6] M.S. Chiou, H.Y. Li, Equilibrium and kinetic modeling of adsorption of reactive dye on crosslinked chitosan beads, J. Hazard. Mater., 93 (2002) 233–248.

[7] X.Y. Yang, B. Al-Duri, Application of branched pore diffusion model in the adsorption of reactive dyes on activated carbon, Chem. Eng. J., 83 (2001) 15–23.

[8] M.S. Mottaleb, D. Littlejohn, Application of an HPLC-FTIR modified thermospray interface for analysis of dye samples, Anal. Sci., 17 (2001) 429–434.

[9] S.M. Burkinshaw, O. Kabambe, Attempts to reduce water and chemical usage in the removal of bifunctional reactive dyes from cotton: Part 2 bis(vinyl sulfone), aminochlorotriazine/ vinyl sulfone and bis(aminochlorotriazine/vinyl sulfone) dyes, Dyes Pigm., 88 (2011) 220–229.

[10] P.C. Vandevivere, R. Bianchi, W. Verstraete, Review: Treatment and reuse of wastewater from the textile wet-processing industry: review of emerging technologies, J. Chem. Technol. Biotechnol., 72 (1998) 289–302.

[11] C. O'Neill, F.R. Hawkes, D.L. Hawkes, N.D. Lourenço, H.M. Pinheiro, W. Delée, Colour in textile effluents–sources, measurement, discharge consents and simulation: a review, J. Chem. Technol. Biotechnol., 74 (1999) 1009–1018.

[12] Y. Ho, T. Chiang, Y. Hsueh, Removal of basic dye from aqueous solution using tree fern as a biosorbent, Process Biochem., 40 (2005) 119–124.

[13] F. Derbyshire, M. Jagtoyen, R. Andrews, A. Rao, I. MartinGullon, E. Grulke, Carbon Materials in Environmental Applications, L.R. Radovic, Ed., Chemistry and Physics of Carbon, Vol. 27, Marcel Dekker, New York, NY, 2001, pp. 1–66.

[14] G. Crini, Non-conventional low-cost adsorbents for dye removal: a review, Bioresour. Technol., 97 (2006) 1061–1085.

[15] L.D. Fiorentin, D.E.G. Trigueros, A.N. Módenes, F.R. Espinoza-Quiñones, N.C. Pereira, S.T.D. Barros, O.A.A. Santos, Biosorption of reactive blue 5G dye onto drying orange bagasse in batch system: kinetic and equilibrium modeling, Chem. Eng. J., 163 (2010) 68–77.

[16] C.P. Kaushik, R. Tuteja, N. Kaushik, J.K. Sharma, Minimization of organic chemical load indirect dyes effluent using low cost adsorbents, Chem. Eng. J., 155 (2009) 234–240.

[17] G.Z. Kyzas, A decolorization technique with spent "Greek Coffee" Grounds as zero-cost adsorbents for industrial textile wastewaters, Materials, 5 (2012) 2069–2087.

[18] G.Z. Kyzas, M. Kostoglou, A.A. Vassiliou, N.K. Lazaridis, Treatment of real effluents from dyeing reactor: experimental and modeling approach by adsorption onto chitosan, Chem. Eng. J., 168 (2011) 577–585.

[19] G.Z. Kyzas, N.K. Lazaridis, A.C. Mitropoulos, Removal of dyes from aqueous solutions with untreated coffee residues as potential low-cost adsorbents: Equilibrium, reuse and thermodynamic approach, Chem. Eng. J., 189–190 (2012) 148–159.

[20] R.S. Juang, R.L. Tseng, F.C. Wu, S.H. Lee, Adsorption behavior of reactive dyes from aqueous solutions on Chitosan, J. Chem. Technol. Biotechnol., 70 (1997) 391–399.

[21] D. Knorr, Dye binding properties of chitin and chitosan, J. Food Sci., 48 (1983) 36–37.

[22] G. Annadurai, L.Y. Ling, J.F. Lee, Adsorption of reactive dye from an aqueous solution by Chitosan: isotherm, kinetic and thermodynamic analysis, J. Hazard. Mater., 152 (2008) 337–346.

[23] S. Chatterjee, S. Chatterjee, B.P. Chatterjee, A.K. Guha, Adsorptive removal of congo red, a carcinogenic textile dye by chitosan hydrobeads: binding mechanism, equilibrium and kinetics, Colloids Surf., A, 299 (2007) 146–152.

[24] F.A.A. Tirkistani, Thermal analysis of some chitosan Schiff bases, Polym. Degrad. Stab., 60 (1998) 67–70.

[25] J.E. dos Santos, E.R. Dockal, E´.T.G. Cavalheiro, Synthesis and characterization of Schiff bases from chitosan and salicylaldehyde derivatives, Carbohydr. Polym., 60 (2005) 277–282.

[26] A.M. Donia, A.A. Atia, K.Z. Elwakeel, Selective separation of mercury(II) using magnetic chitosan resin modified with Schiff's base derived from thiourea and glutaraldehyde, J. Hazard. Mater., 151 (2008) 372–379.

[27] H.M. Zalloum, Z. Al-Qodah, M.S. Mubarak, Copper adsorption on chitosan derived schiff bases, J. Macromol. Sci., Part A, 46 (2008) 46–57.

[28] E.A. Soliman, S.M. El-Kousy, H.M. Abd-Elbary, A.R. Abou-Zeid, Low molecular weight chitosan-based Schiff bases: synthesis, characterization and antimicrobial activity, J. Food Technol., 8 (2013) 17–30.

[29] Y.N. Dai, P. Li, J.P. Zhang, A.Q. Wang, Q. Wei, Swelling characteristics and drug delivery properties of nifedipine-loaded pH-sensitive alginate–chitosan hydrogel beads, J. Biomed. Mater. Res., Part B: Appl. Biomater., 86B (2008) 493–500.

[30] S.P. Ramnani, S. Sabharwal, Adsorption behavior of Cr(VI) onto radiation crosslinked Chitosan and its possible application for the treatment of wastewater containing Cr(VI), React. Funct. Polym., 66 (2006) 902–909.

[31] Y.A. Ismail, S.R. Shin, K.M. Shin, S.G. Yoon, K. Shon, S.I. Kim, Electrochemical actuation in chitosan/polyaniline microfibers for artificial muscles fabricated using an in situ polymerization, Sens. Actuat. B, 129 (2008) 834–840.

[32] S.J. Kim, S.G. Yoon, I.Y. Kim, S.I. Kim, Swelling characterization of the semi-interpenetrating polymer network hydrogels composed of chitosan and poly(diallyldimethylammonium chloride), J. Appl. Polym. Sci., 91(2004) 2876–2880.

[33] M. Abedini, F. Shirini, J.M.-A. Omran, M. Seddighi, O. Goli-Jolodar, Succinimidinium N-sulfonic acid hydrogen sulfate as an efficient ionic liquid catalyst for the synthesis of 5-arylmethylene-pyrimidine-2,4,6-trione and pyrano [2,3-d] pyrimidinone derivatives, Res. Chem. Intermed., 42 (2016) 4443–4458.

[34] 2-Pyrrolidinone, 1-methyl, https://webbook.nist.gov/cgi/cbook.cgi?ID=C872504&Mask=80

[35] M.S. Mohy Eldin, A.I. Hashem, A.M. Omer, T.M. Tamer, Preparation, characterization and antimicrobial evaluation of novel cinnamyl chitosan Schiff base, Int. J. Adv. Res., 3 (2015) 741–755.

[36] A. Pawlak, M. Mucha, Thermogravimetric and FTIR studies of chitosan blends, Thermochim. Acta, 396 (2003) 153–166.

[37] M.K. Cheung, K.P.Y. Wan, P.H.J. Yu, Miscibility and morphology of chiral semicrystalline poly-(R)-(3-hydroxybutyrate)/chitosan and poly-(R)-(3-hydroxybutyrate-co-3-hydroxyvalerate)/chitosan blends studied with DSC, ^{1}H T_1 and $T_{1\rho}$ CRAMPS, J. Appl. Polym. Sci., 86 (2002) 1253–1258.

[38] V. Gonzalez, C. Guerrero, U. Ortiz, Chemical structure and compatibility of polyamide–chitin and chitosan blends, J. Appl. Polym. Sci., 78 (2000) 850–857.

[39] F.S. Kittur, H. Prashanth, K.U. Sankar, R.N. Tharanathan, Characterization of chitin, chitosan and their carboxymethyl derivatives by differential scanning calorimetry, Carbohydr. Polym., 49 (2002) 185.

[40] T.M. Tamer, M.A. Hassan, A.M. Omer, K. Valachová, M.S. Mohy Eldin, M.N. Collins, L. Šoltés, Antibacterial and antioxidative activity of O-amine functionalized chitosan, Carbohydr. Polym., 169 (2017) 441–450.

[41] M. Hema, S. Arivoli, Comparative study on the adsorption kinetics and thermodynamics of dyes onto acid-activated low cost carbon, Int. J. Phys. Sci., 2 (2007) 10–17.
[42] I.A.W. Tan, B.H. Hameed, A.L. Ahmad, Equilibrium and kinetic studies on basic dye adsorption by oil palm fibre activated carbon, Chem. Eng. J., 127(2007) 111–119.
[43] B. Noroozi, G.A. Sorial, H. Bahrami, M. Arami, Equilibrium and kinetic adsorption study of a cationic dye by a natural adsorbent—Silkworm pupa, J. Hazard. Mater., 39 (2007) 167–174.
[44] I. Uzun, Kinetics of the adsorption of reactive dyes by chitosan, Dyes Pigm., 70 (2006) 76–83.
[45] H. Hou, R. Zhou, P. Wu, L. Wu, Removal of Congo red dye from aqueous solution with hydroxylapatite/chitosan composite, Chem. Eng. J., 211–212 (2012) 336–342.
[46] A. Szyguła, E. Guibal, M.A. Palacın, M. Ruiz, A.M. Sastre, Removal of an anionic dye (Acid Blue 92) by coagulation-flocculation using chitosan, J. Environ. Manage., 90 (2009) 2979–2986.
[47] M.S. Chiou, H.O. Pang-Yen, H.-Y. Li, Adsorption of anionic dyes in acid solutions using chemically crosslinked chitosan beads, Dyes Pigm., 60 (2004) 69–84.
[48] E.M. El-Sayed, T.M. Tamer, A.M. Omer, M.S. Mohy Eldin, Development of novel chitosan schiff base derivatives for cationic dye removal: methyl orange model, Desal. Water Treat., 57 (2016) 22632–22645.
[49] C. Nhamo, C.M. Edna, G. Willis, Synthesis, characterization and methyl orange adsorption capacity of ferric oxide–biochar nanocomposites derived from pulp and paper sludge, Appl Water Sci., 7 (2017) 2175–2186.
[50] F. Falaki, A. Fakhri, Study of the adsorption of methyl orange from aqueous solution using nickel oxide nanoparticles: equilibrium and kinetics studies, J. Phys. Theor. Chem., 10 (2013) 117–124.
[51] J. Ma, M. Yao, Y. Fei, A novel one-pot route for large-scale synthesis of novel magnetic CNTs/Fe@C hybrids and their applications for binary dye removal, Sustainable Chem. Eng., 6 (2018) 8178–8191.
[52] A. Ahmad, M.H. Razali, M. Mamat, F.S.B. Mehamod, K.A.M. Amin, Adsorption of methyl orange by synthesized and functionalized-CNTs with 3-aminopropyltriethoxysilane loaded TiO_2 nanocomposites, Chemosphere, 168 (2017) 474–482.